

Self-consistent simulation studies of periodically focused intense charged-particle beams

C. Chen

Plasma Fusion Center, Massachusetts Institute of Technology, Cambridge, Massachusetts 02139

R. A. Jameson

Accelerator Operations and Technology Division, Los Alamos National Laboratory, Los Alamos, New Mexico 87545

(Received 27 March 1995)

A self-consistent two-dimensional model is used to investigate intense charged-particle beam propagation through a periodic solenoidal focusing channel, particularly in the regime in which there is a mismatch between the beam and the focusing channel. The present self-consistent studies confirm that mismatched beams exhibit nonlinear resonances and chaotic behavior in the envelope evolution, as predicted by an earlier envelope analysis [C. Chen and R. C. Davidson, *Phys. Rev. Lett.* **72**, 2195 (1994)]. Transient effects due to emittance growth are studied, and halo formation is investigated. The halo size is estimated. The halo characteristics for a periodic focusing channel are found to be qualitatively the same as those for a uniform focusing channel. A threshold condition is obtained numerically for halo formation in mismatched beams in a uniform focusing channel, which indicates that relative envelope mismatch must be kept well below 20% to prevent space-charge-dominated beams from developing halos.

PACS number(s): 07.77.+p, 29.27.Eg, 41.75.-i, 52.25.Wz

I. INTRODUCTION

There has been considerable interest in advanced high-current ion accelerators for a variety of applications ranging from heavy ion fusion [1,2] to accelerator production of tritium [3]. The most important milestone in the development of such high-average-power ion beam systems is to accelerate and transport space-charge-dominated ion beams with extremely low beam loss. One mechanism for beam losses is attributed to mismatch between the beam and the focusing system, because a mismatched beam causes a halo to develop [4–8] which may make physical contact with some components of the system. Practical difficulties of achieving precise beam matching have motivated, in recent years, vigorous theoretical and experimental investigations [4–6,9–15] of the effects of mismatch on the dynamics of space-charge-dominated beams.

Several theoretical investigations of mismatched, space-charge-dominated beams have been carried out using root-mean-squared (rms), test-particle, and self-consistent particle-in-cell (PIC) models. In particular, it has been predicted in an envelope analysis [9–11] that, for a periodic solenoidal focusing configuration, the beam self-fields induce a rich variety of nonlinear resonances and chaotic behavior in the beam envelope oscillations. It has also been shown in test-particle analyses that particle orbits themselves can become chaotic either due to beam density nonuniformities [12,13] for an alternating-gradient quadrupole focusing configuration or due to mismatched envelopes [14,15] for an axisymmetric uniform focusing configuration. Moreover, self-consistent PIC computer simulations [4,5] have shown that an

envelope-mismatched beam can form a dense core and a tenuous halo, via an array of nonlinear resonances and chaotic processes in the beam dynamics. However, few comparisons have been made between these analyses and self-consistent simulations.

In this paper, a self-consistent two-dimensional macro-particle model is presented for space-charge-dominated charged-particle beams and is used to investigate the evolution of both rms beam quantities and the particle phase-space distribution, particularly in the regime where a mismatch between the beam and the focusing channel occurs. The present investigation is concentrated on a periodic solenoidal focusing channel which possesses axisymmetry. It is demonstrated in the benchmark simulations that, with as many as 10^3 macroparticles in the present model, the properties of stable Kapchinskij-Vladimirskij (KV) beam equilibria [10,16–18] are preserved over propagating distances at least on the order of 100 focusing periods. As predicted by the previous envelope analysis [9–11], nonlinear resonant and chaotic phenomena in the envelope evolution are confirmed in the computer simulations, supporting the expectation that such nonlinear phenomena should be experimentally observable. Halo formation is investigated. While the analytical model [14,15] for envelope-mismatched beams without emittance growth does not provide an escape mechanism for core particles to move into the halo, the emittance growth and transient effects in the self-consistent model provide escape mechanisms. The size of the halo is estimated. The halo characteristics for periodic focusing configurations are found to be qualitatively the same as those for uniform focusing configurations. A threshold condition for halo formation is obtained numerically.

II. THE MACROPARTICLE MODEL

We consider a thin, continuous, intense charged-particle beam propagating with average axial velocity $\beta_b c \vec{e}_z$ through an axisymmetric, linear focusing channel provided by the applied, periodic solenoidal magnetic field

$$\vec{B}_0(x, y, s) = B_z(s) \vec{e}_z - \frac{1}{2} B'_z(s) (x \vec{e}_x + y \vec{e}_y) \quad (1)$$

and

$$\vec{B}_0(x, y, s + S) = \vec{B}_0(x, y, s), \quad (2)$$

where $s = z$ is the axial coordinate, S is the fundamental periodicity length of the focusing field, the "prime" denotes derivative with respect to s , and c is the speed of light *in vacuo*.

In the present self-consistent two-dimensional macroparticle model, the beam is represented by N_p macroparticles. The beam density is approximated by

$$n(x, y, s) = \frac{N}{N_p} \sum_{i=1}^{N_p} \delta(x - x_i(s)) \delta(y - y_i(s)), \quad (3)$$

where $N = \int n(x, y, s) dx dy = \text{const}$ is the number of microparticles per unit axial length of the beam, (x_i, y_i) is the transverse position of the i th macroparticle, and $\delta(x)$ is the Dirac δ function. Under the paraxial approximation [10,18], the self-electric and self-magnetic fields associated with the beam space-charge and current are expressed as

$$\vec{E}^{(s)}(x, y, s) = - \left[\vec{e}_x \frac{\partial}{\partial x} + \vec{e}_y \frac{\partial}{\partial y} \right] \Phi^{(s)}(x, y, s), \quad (4)$$

and

$$\vec{B}^{(s)}(x, y, s) = \left[\vec{e}_x \frac{\partial}{\partial y} - \vec{e}_y \frac{\partial}{\partial x} \right] A_z^{(s)}(x, y, s), \quad (5)$$

where the scalar potential for the self-electric field obeys the Poisson equation

$$\left[\frac{\partial^2}{\partial x^2} + \frac{\partial^2}{\partial y^2} \right] \Phi^{(s)}(x, y, s) = -4\pi q n(x, y, s), \quad (6)$$

and the vector potential for the self-magnetic field is defined by

$$\vec{A}^{(s)}(x, y, s) = \beta_b \Phi^{(s)}(x, y, s) \vec{e}_z. \quad (7)$$

Here q is the particle charge.

For such a beam of N_p macroparticles moving in the combined periodic solenoidal and self-fields $\vec{E}^{(s)}$ and $\vec{B}_0 + \vec{B}^{(s)}$, the transverse equations of motion for the i th macroparticle can be expressed as [10,18]

$$\begin{aligned} \frac{d^2 x_i}{ds^2} - 2\sqrt{\kappa_z(s)} \frac{dy_i}{ds} - \left[\frac{d}{ds} \sqrt{\kappa_z(s)} \right] y_i \\ + \frac{q}{\gamma_b^3 \beta_b^2 mc^2} \frac{\partial}{\partial x_i} \Phi^{(s)}(x_i, y_i) = 0 \end{aligned} \quad (8)$$

and

$$\begin{aligned} \frac{d^2 y_i}{ds^2} + 2\sqrt{\kappa_z(s)} \frac{dx_i}{ds} + \left[\frac{d}{ds} \sqrt{\kappa_z(s)} \right] x_i \\ + \frac{q}{\gamma_b^3 \beta_b^2 mc^2} \frac{\partial}{\partial y_i} \Phi^{(s)}(x_i, y_i) = 0, \end{aligned} \quad (9)$$

where $i = 1, 2, \dots, N_p$, m is the particle rest mass, $\gamma_b = (1 - \beta_b^2)^{-1/2}$ is the relativistic mass factor,

$$\sqrt{\kappa_z(s)} = \frac{q B_z(s)}{2\gamma_b \beta_b mc^2} \quad (10)$$

is the focusing parameter, and

$$\begin{aligned} \Phi^{(s)}(x_i, y_i) = \frac{qN}{4\pi N_p} \sum_{j=1(j \neq i)}^{N_p} \ln[(x_i - x_j)^2 \\ + (y_i - y_j)^2] \end{aligned} \quad (11)$$

is the scalar potential experienced by the i th macroparticle and is obtained from Eqs. (3) and (6).

As described by Eqs. (8)–(11), the self-consistent two-dimensional macroparticle model for intense charged-particle beams involves $2N_p$ second-order ordinary differential equations which can be integrated numerically with a computer code. The present macroparticle (direct interaction) model, which is equivalent to particle-in-cell (PIC) models, is more straightforward but requires more computations than corresponding PIC models.

It should be recalled that the total emittance [19] of a KV beam in a solenoidal focusing channel is defined by

$$\epsilon_x = 4(\langle \bar{x}^2 \rangle \langle \bar{x}'^2 \rangle - \langle \bar{x} \bar{x}' \rangle^2)^{1/2}, \quad (12)$$

$$\epsilon_y = 4(\langle \bar{y}^2 \rangle \langle \bar{y}'^2 \rangle - \langle \bar{y} \bar{y}' \rangle^2)^{1/2}, \quad (13)$$

for the \bar{x} and \bar{y} directions, respectively; i.e., four times the rms emittance. In Eqs. (12) and (13), $\langle \rangle$ denotes the ensemble average over the beam particle distribution. The coordinate in the Larmor frame [20] of reference, (\bar{x}, \bar{y}) , is related to the coordinate in the laboratory frame of reference, (x, y) , by the relations

$$\bar{x}(s) = x(s) \cos[\phi(s)] - y(s) \sin[\phi(s)], \quad (14)$$

$$\bar{y}(s) = x(s) \sin[\phi(s)] + y(s) \cos[\phi(s)], \quad (15)$$

where $\phi(s) = \int_{s_0}^s ds \sqrt{\kappa_z(s)}$.

It is inevitable that roundoff errors and discrete particle effects generate noise in computer simulations of charged-particle beams, regardless of whether the present macroparticle model or a PIC model is used. Therefore it is important to validate simulation results, which is done in part by simulating beam propagation with the matched KV equilibrium distribution. The KV equilibrium [16–18] is the only known Vlasov equilibrium for periodically focused intense charged-particle beams and has been discussed extensively [10] for the periodic solenoidal magnetic field configuration. In the configuration space, a stable KV beam equilibrium corresponds to a solid beam with a uniform transverse density profile and a radius which varies periodically in the direction of propa-

gation with the same periodicity as the focusing lattice.

It is demonstrated in our benchmark simulations that, with as many as 10^3 macroparticles in the present model, the properties of stable KV beam equilibria are preserved over propagating distances at least on the order of 100 focusing periods. In particular, the computer simulations show that the particles are well confined within the periodically varying outermost beam envelope, and that the beam emittance remains constant within expected relative fluctuations of order of $N_p^{-1/2}$. For a KV equilibrium in a periodic solenoidal channel [10], note that the beam is *round* with uniform density and $\epsilon_{\bar{x}} = \epsilon_{\bar{y}}$, and that the constants $\pi\epsilon_{\bar{x}}$ and $\pi\epsilon_{\bar{y}}$ are equal to the areas occupied uniformly by the beam particles in the phase planes (\bar{x}, \bar{x}') and (\bar{y}, \bar{y}') , respectively.

III. DYNAMICS OF MISMATCHED BEAMS

The beam self-fields induce a rich variety of nonlinear resonances and chaotic behavior in the envelope oscillations of mismatched, space-charge-dominated beams propagating through a periodic solenoidal focusing channel. This was first predicted based on an envelope analysis [9,10] in which the beam emittance was assumed to be constant and the effect of emittance growth was ignored. In this section, we verify the predicted results and study the particle phase-space distribution, using the present macroparticle model which allows for the self-consistent evolution of the beam emittance.

In the remainder of this article, we introduce the dimensionless variables and parameters defined by

$$\begin{aligned} \frac{s}{S} \rightarrow s, \quad \frac{x}{\sqrt{\epsilon_0 S}} \rightarrow x, \quad \frac{y}{\sqrt{\epsilon_0 S}} \rightarrow y, \\ S^2 \kappa_z \rightarrow \kappa_z, \quad \frac{SK}{\epsilon_0} \rightarrow K, \end{aligned} \quad (16)$$

where $\epsilon_0 = \epsilon_{\bar{x}}(0) = \epsilon_{\bar{y}}(0)$ is the initial total KV beam emittance which is assumed to be the same for the \bar{x} and \bar{y} directions. Unless specified otherwise, the above dimensionless variables and parameters will be used hereafter.

To make direct comparisons with the earlier envelope analysis [9–11], we consider here a specific periodic focusing channel described by

$$\kappa_z(s) = [a_0 + a_1 \cos(2\pi s)]^2. \quad (17)$$

The vacuum phase advance over one period of such a focusing lattice is given approximately by

$$\sigma_0 = \left[\int_0^1 \kappa_z(s) ds \right]^{1/2} = \left[a_0^2 + \frac{a_1^2}{2} \right]^{1/2}. \quad (18)$$

Furthermore, we define the effective (total) beam radius as

$$r_b = \sqrt{2 \langle r^2 \rangle} = \sqrt{2 \langle x^2 + y^2 \rangle}, \quad (19)$$

which is $\sqrt{2}$ times the rms beam radius $\langle r^2 \rangle^{1/2}$. For the special case of the matched KV equilibrium distribution [10], the effective beam radius is equal to the outermost

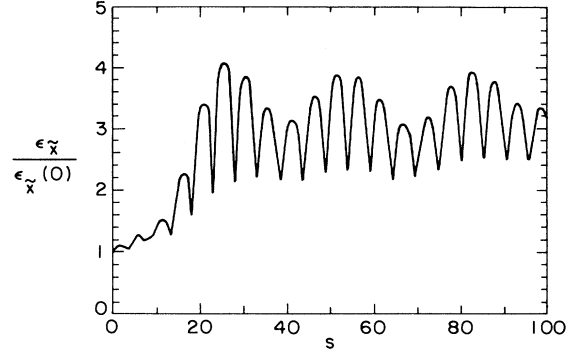


FIG. 1. Evolution of the relative rms emittance of a mismatched, space-charge-dominated beam in the focusing channel, as obtained from the simulation for the following choice of parameters: $K=3$, $a_0=a_1=0.648$ ($\sigma_0=45.5^\circ$), $\delta r_b/\bar{r}_b(0)=0.75$, and $N_p=1024$.

beam radius, because the beam is round with uniform density.

A. Nonlinear resonances and chaotic behavior in the rms evolution

Figures 1 and 2 show, respectively, the evolution of the emittance and effective radius [computed as rms quantities using Eqs. (12), (13), and (19)], of a mismatched, space-charge-dominated beam propagating through the focusing channel, as obtained from the simulation for the following choice of system parameters: $K=3$, $a_0=a_1=0.648$ ($\sigma_0=45.5^\circ$), and $N_p=1024$. The beam is loaded initially according to a KV distribution but the beam radius is mismatched outward initially by 75% from the equilibrium beam radius, i.e., $\delta r_b = r_b(0) - \bar{r}_b(0)$ is the initial beam radius mismatch and $\bar{r}_b(0)$ is the initial beam radius of the corresponding matched KV beam equilibrium. It is evident in Fig. 1 that the emittance $\epsilon_{\bar{x}}$ varies significantly as the beam propagates through the focusing channel. When

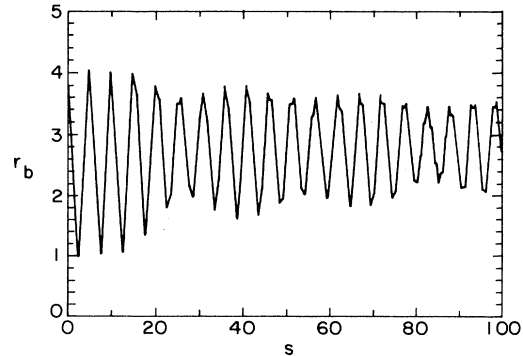


FIG. 2. Evolution of the effective beam radius for a mismatched, space-charge-dominated beam in the focusing channel, as obtained from the simulation for the same choice of system parameters shown in Fig. 1.

the emittance reaches its maximum at $s \cong 23$, it has increased by as much as a factor of three from its initial value. The emittance for the \bar{y} direction evolves in a similar way as that for the \bar{x} direction. As a result of emittance growth, transient effects are observed in the envelope evolution shown in Fig. 2, particularly in the early stage of development from $s=0$ to 25. Both the emittance and the effective beam radius oscillate back and forth once approximately every five lattice periods. The oscillation period is given approximately by [9]

$$\lambda = 2\pi[4\sigma_0^2 + K^2 - K(4\sigma_0^2 + K^2)^{1/2}]^{-1/2}. \quad (20)$$

Because the beam emittance increases on average by a factor of two from its initial value, the effective value of K is $K=1.0$ for the case shown in Fig. 2. Substituting $\sigma_0=45.5^\circ$ and $K=1.0$ into Eq. (20) yields the oscillation period $\lambda=4.9$ (i.e., 4.9 lattice periods), which is in good agreement with the simulation result.

From the data shown in Fig. 2, the effective beam radius is differentiated with respect to s , and the Poincaré surface-of-section plot [21] is generated to better visualize the resonant behavior in the envelope oscillations. The result is the separatrix of the fifth-order nonlinear resonance shown in Fig. 3, where the effective beam radius r_b and its derivative $r'_b = dr_b/ds$ are plotted in the plane (r_b, r'_b) at $s=26, 27, \dots, 75$. For a clear view of the nonlinear resonance structure, the 50 points in Fig. 3 are connected by five contours, each of which traces ten points that are separated longitudinally by about five lattice periods with random fluctuations seen typically inside a chaotic, slightly broadened separatrix. A chain of five stable islands is found inside the five contours shown in Fig. 3. This result agrees qualitatively with the earlier prediction based on the envelope analysis, as one compares present Fig. 3 with Fig. 2(b) in [9]. Both analyses show weakly chaotic behavior in the envelope evolution. (Note that the overall structure of the nonlinear resonance depends crucially on σ_0 and K [9] but does not change qualitatively from a sinusoidal to step-function focusing lattice.) Although not shown in present Fig. 3, a fourth-order nonlinear resonance is also found for larger

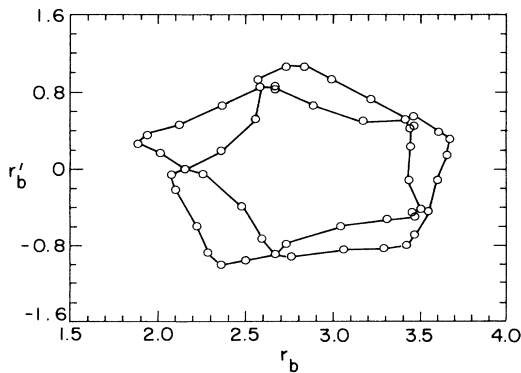


FIG. 3. Poincaré surface-of-section plot generated from the data in Fig. 2 showing the separatrix of the fifth-order nonlinear resonance for the envelope evolution from $s=26$ to 75.

initial envelope mismatches [e.g., $\delta r_b / \bar{r}_b(0) = 1.6$], as predicted by the earlier envelope analysis. Of course, the main advantage in the present analysis is that the beam emittance is allowed to evolve self-consistently. More importantly, the simulation results presented in Figs. 1–3 show that, after emittance growth and transient effects, the nonlinear resonances and chaotic behavior in the envelope evolution should be experimentally observable for mismatched, space-charge-dominated beams propagating through a periodic focusing channel.

Although more pronounced chaotic behavior was predicted in the envelope oscillations for $\sigma_0 > 90^\circ$ [9–11], a direct confirmation of such chaotic envelope oscillations remains challenging. This is because emittance growth is found to be so pronounced in this regime that initially space-charge-dominated beams tend to evolve rapidly into emittance-dominated beams.

B. Evolution of the particle distribution and halo formation

The rms properties of mismatched, space-charge-dominated beams vary smoothly and exhibit nonlinear resonances and weakly chaotic behavior, as discussed in Sec. III A. Once mismatch causes a beam to form a dense core and a tenuous halo, however, the rms description of the beam becomes inadequate. Under such circumstances, we must also examine the self-consistent evolution of the beam particle distribution in the phase space (x, y, x', y') . From the point of view of accelerator design, of particular interest are the condition for halo formation and the size of a beam halo relative to the effective beam radius.

Shown in Fig. 4 are plots of the particle phase plane (x, y) at (a) $s=38$, (b) $s=39$, (c) $s=40$, (d) $s=41$, (e) $s=42$, and (f) $s=43$, for the same choice of system parameters shown in Figs. 1–3. Approximately 5% of macroparticles are in the beam halo. The halo radius (i.e., maximum radius achieved by halo particles) is approximately constant as the beam propagates through the focusing channel. The ratio of the halo radius to the maximum effective beam radius is found to be about 1.6, as seen from Figs. 2 and 4(d), whereas the ratio of the halo radius to the minimum effective beam radius is about 3.8, as seen from Figs. 2 and 4(a).

It is found that the characteristics of halos do not change qualitatively from a periodic to uniform focusing channel. This is perhaps because the focusing parameter of a periodic focusing channel $\kappa_z(s)$ may be averaged over one focusing period to yield a uniform focusing channel with the effective (dimensional) focusing parameter $\kappa_{z0} = \int_0^S \kappa_z(s) ds = (\sigma_0/S)^2 = \text{const}$.

Finally, we estimate the mismatch threshold for halo formation by means of computer simulations. For simplicity, this is done for the case of an initially KV distribution propagating through a uniform focusing channel with $\kappa_z(s) = \text{const}$. In such a simulation, the maximum radius achieved by the beam particles is determined after the beam has propagated more than 50 periods of mismatched envelope oscillations. The simulations are

performed over a wide range of K and $\delta r_b/\bar{r}_b$, where $\delta r_b = r_b(0) - \bar{r}_b \geq 0$, $r_b(0)$ is the initial beam radius, and $\bar{r}_b = \text{const}$ is the radius for the matched beam in the uniform focusing channel. The results are shown in Figs. 5 and 6, where the maximum radius achieved by the beam particles r_m is plotted relative to the initial beam radius $r_b(0)$ as a two-dimensional function of the relative mismatch amplitude $\delta r_b/\bar{r}_b$ and the space-charge param-

eter $\mu = 1 - (\sigma/\sigma_0)^2$. Here, σ_0 and $\sigma = (1/2)[(K^2 + 4\sigma_0^2)^{1/2} - K]$ are the vacuum and space-charge-depressed phase advances per unit axial length for the matched beam, respectively. Note that $\mu \rightarrow 1$ ($K/\sigma_0 \gg 1$) for space-charge-dominated beams, whereas $\mu \rightarrow 0$ ($K/\sigma_0 \rightarrow 0$) for emittance-dominated beams.

The onset of a plateau in Fig. 5 defines the threshold for halo formation, which occurs at $\delta r_b/\bar{r}_b \cong 0.2$ for

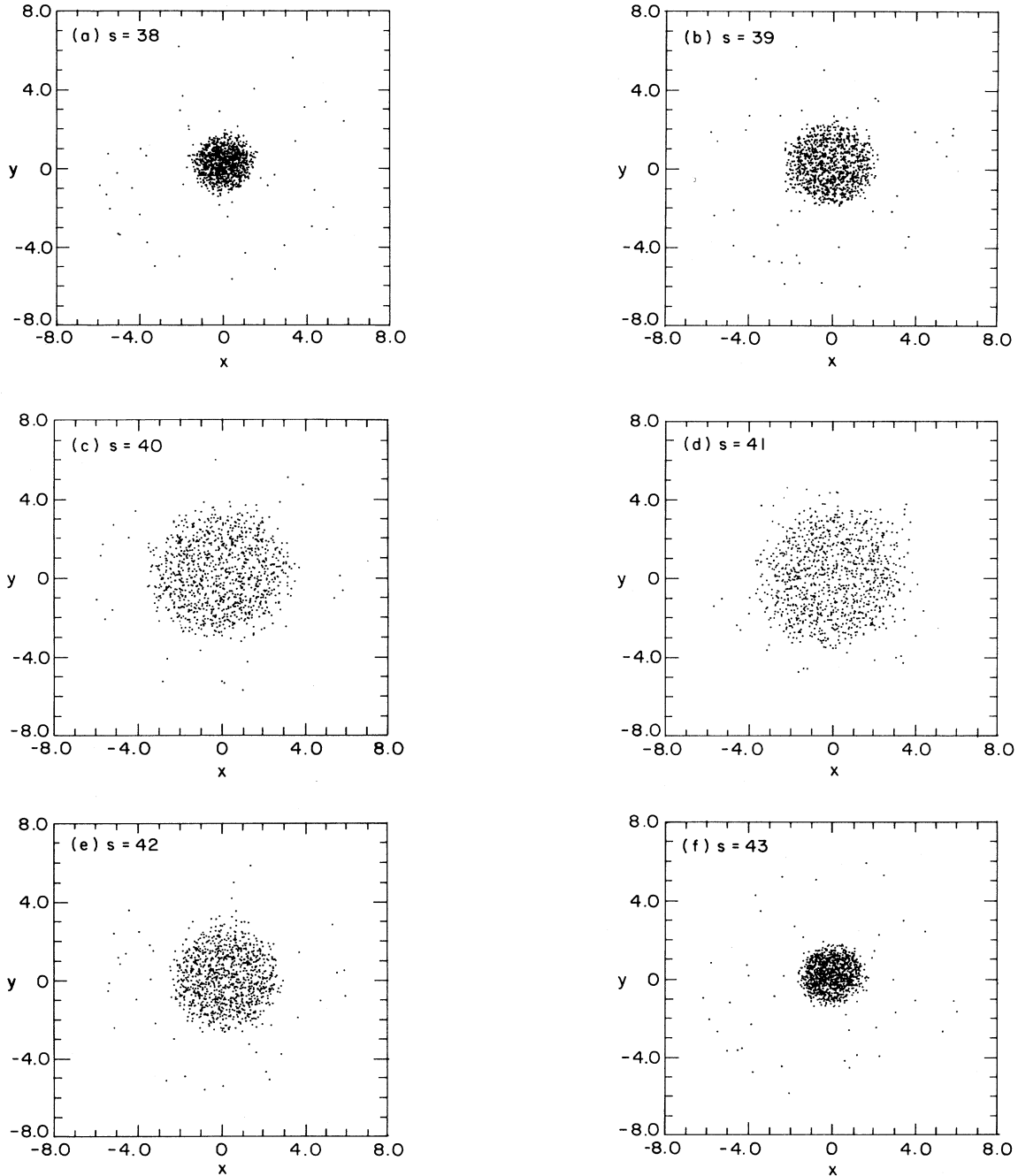


FIG. 4. Plots of 1024 macroparticles in the phase plane (x, y) at (a) $s = 38$, (b) $s = 39$, (c) $s = 40$, (d) $s = 41$, (e) $s = 42$, and (f) $s = 43$, for the same choice of system parameters shown in Figs. 1–3.

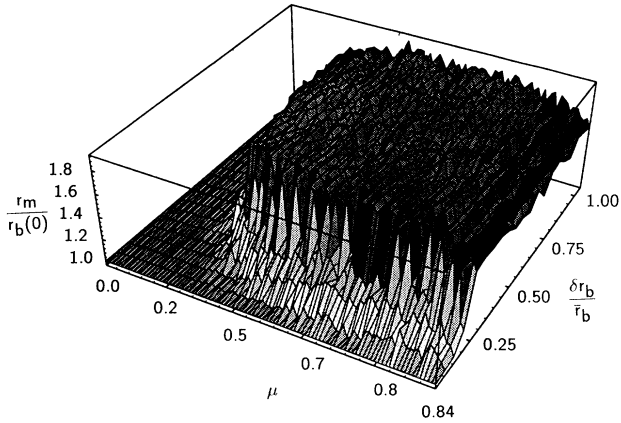


FIG. 5. Relative maximum radius $r_m/r_b(0)$ achieved by the beam particles as a two-dimensional function of the relative mismatch amplitude $\delta r_b/\bar{r}_b$ and the space-charge parameter $\mu = 1 - (\sigma/\sigma_0)^2$, obtained from simulations for the case of a uniform focusing channel.

$\mu > 0.4$ but becomes increasingly large as $\mu \rightarrow 0$, as indicated by the dense contours in Fig. 6. The plateau shown in Fig. 5 is approximately flat and has a vertical height of $r_m/r_b(0) \cong 1.6$, which is in agreement with the results shown in Figs. 2 and 4(d). The contour plot shown in Fig. 6 reveals fine structures associated with various nonlinear resonances and chaotic processes in the beam dynamics. Similar and more detailed results have also been reported in [4,5] for an initially Hamiltonian distribution [22] in a uniform focusing channel.

IV. CONCLUSIONS

A self-consistent two-dimensional macroparticle model was presented for studies of the dynamics of intense charged-particle beams propagating through an axisymmetric, linear focusing channel provided by a periodic solenoidal magnetic field. It was demonstrated in the benchmark simulations that, with as many as 10^3 macroparticles in the present model, the properties of stable KV beam equilibria are preserved over propagating distances at least on the order of 100 focusing periods.

The self-consistent evolution of the rms quantities such as the rms envelope and emittance was investigated in the space-charge-dominated regime. It was confirmed in the computer simulations that, for beams mismatched into the periodic focusing channel, the beam envelope exhibits nonlinear resonances and chaotic behavior, as predicted by the previous analysis of the beam envelope equation [9–11]. As a result of emittance growth, transient effects were observed in the rms beam evolution. These results further support the expectation that the nonlinear reso-

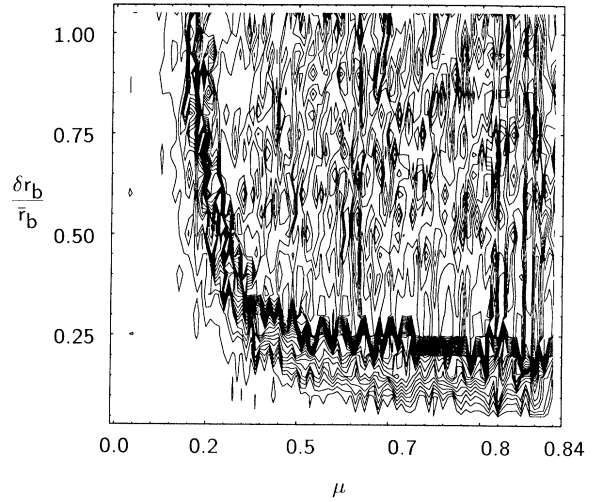


FIG. 6. Shown in a contour plot the same data in Fig. 5 for a clear view of fine structures. Here, two adjacent contours are separated by $\Delta r_m/r_b(0) = 0.02$. The onset of the plateau (i.e., threshold for halo formation) is indicated by the dense contours located approximately at $\delta r_b/\bar{r}_b = 0.2$ for $\mu > 0.4$.

nances and chaotic behavior in the envelope evolution should be experimentally observable after the emittance growth and transient effects for mismatched, space-charge-dominated beams propagating through a periodic focusing channel.

Also investigated were the self-consistent evolution of the particle distribution in the phase space and halo formation. Unlike the analytical model [14,15] for envelope-mismatched beams without emittance growth which does not provide an escape mechanism for core particles to move into the halo, the emittance growth and transient effects in the self-consistent model provided escape mechanisms. The halo size was estimated. The halo characteristics for a periodic focusing channel were found to be qualitatively the same as those for a uniform focusing channel. A threshold condition was obtained numerically for halo formation for mismatched beams in the uniform focusing channel, which indicates that relative envelope mismatch must be kept well below 20% in order to prevent space-charge-dominated beams from developing halos.

ACKNOWLEDGMENTS

This work was supported in part by the Department of Energy, Office of High Energy and Nuclear Physics, Grant No. DE-FG02-95ER40919 and in part by the Air Force Office of Scientific Research, Grant No. F46920-94-1-0374.

[1] R. W. Müller, in *Nuclear Fusion by Inertial Confinement: A Comprehensive Treatise*, edited by G. Velarde, Y. Ronen, and J. M. Martinez-Val (CRC, Boca Raton, FL, 1993), p. 437.

[2] *Heavy Ion Inertial Fusion*, edited by M. Reiser, T. Godlove, and R. Bangerter, AIP Conf. Proc. No. 152 (AIP, New York, 1986).

[3] R. A. Jameson, in *Advanced Accelerator Concepts*, edited

- by J. S. Wurtele, AIP Conf. Proc. No. 279 (AIP, New York, 1993).
- [4] R. A. Jameson, Los Alamos National Laboratory Report No. LA-UR-93-1209, 1993 (unpublished); *Proceedings of the 1993 Particle Accelerator Conference* (IEEE Service Center, Piscataway, NJ, 1993), Vol. 5, p. 3936.
- [5] R. A. Jameson, Los Alamos National Laboratory Report No. LA-UR-94-3753, 1994 (unpublished).
- [6] D. Kehne, M. Reiser, and H. Rudd, in *Proceedings of the 1991 Particle Accelerator Conference* (IEEE Service Center, Piscataway, NJ, 1991), Vol. 1, p. 248; A. Cucchetti, M. Reiser, and T. Wangler, in *ibid.*, p. 251.
- [7] Los Alamos Scientific Laboratory Report No. LA-UR-7265-C, 1978 (unpublished).
- [8] R. A. Jameson, R. S. Mills, and O. R. Sander, Los Alamos National Laboratory Report No. LA-UR-92-3033, 1992 (unpublished).
- [9] C. Chen and R. C. Davidson, *Phys. Rev. Lett.* **72**, 2195 (1994).
- [10] C. Chen and R. C. Davidson, *Phys. Rev. E* **49**, 5679 (1994).
- [11] S. Y. Lee and A. Riabko, *Phys. Rev. E* **51**, 1609 (1995).
- [12] Q. Qian, R. C. Davidson, and C. Chen, *Phys. Plasmas* **1**, 3104 (1994).
- [13] Q. Qian, R. C. Davidson, and C. Chen, *Phys. Rev. E* **51**, 5216 (1995); *Phys. Plasmas* **2**, 2674 (1995).
- [14] J. S. O'Connell, T. P. Wangler, R. S. Mills, and K. R. Crandall, in *Proceedings of the 1993 Particle Accelerator Conference* (IEEE Service Center, Piscataway, NJ, 1993), Vol. 5, p. 3657.
- [15] R. L. Gluckstern, *Phys. Rev. Lett.* **73**, 1247 (1994).
- [16] I. M. Kapchinskij and V. V. Vladimirkij, *Proceedings International Conference on High Energy Accelerators* (CERN, Geneva, 1959), p. 274.
- [17] I. Hofmann, L. J. Laslett, L. Smith, and I. Haber, *Part. Accel.* **13**, 145 (1983).
- [18] R. C. Davidson, *Physics of Nonneutral Plasmas* (Addison-Wesley, Reading, MA, 1990), Chap. 10.
- [19] P. M. Lapostolle, *IEEE Trans. Nucl. Sci.* **NS-18**, 1101 (1971).
- [20] J. D. Lawson, *Physics of Charged-Particle Beams* (Oxford Science, New York, 1988).
- [21] A. J. Lichtenberg and M. A. Leiberman, *Regular and Chaotic Dynamics*, 2nd ed. (Springer-Verlag, New York, 1992).
- [22] R. L. Gluckstern, R. Mills, and K. Crandall (unpublished).